Effects of Uniaxial Stress on the Electrical Resistivity and the Gunn Effect in n-Type GaAs

J. S. Harris,* J. L. Moll,† AND G. L. Pearson

Stanford Electronic Laboratories, Stanford University, Stanford University, Stanford, California 94305

(Received 2 October 1969)

Electrical resistivity and Gunn-effect threshold measurements as a function of uniaxial stress were made on horizontal boat-grown GaAs and liquid epitaxial GaAs. The electron concentration of the boat-grown material exhibited an exponential change with both temperature and stress. The exponential behavior is characteristic of a semiconductor in which the electrical properties are dominated by deep trap levels. The electron concentration of the epitaxial GaAs remained nearly constant with both temperature and stress. For $\langle 100 \rangle$ stresses greater than 9 kbar, the resistivity increased rapidly and the current oscillations at high electric fields were quenched. However, the resistivity and current oscillations remained nearly constant when large $\langle 111 \rangle$ stresses were applied. Thus, the $\langle 100 \rangle$ or X_1 valleys are the important valleys for electron transfer at high electric fields. The deformation potentials obtained for the X_1 valleys are $\Xi_u^1 = 16.8$ eV/(unit strain), $\Xi_d^1 = -5.1$ eV/(unit strain), and, for the $\langle 000 \rangle$ or Γ_1 valley, $\Xi_d^0 = 7.8$ eV/(unit strain).

I. INTRODUCTION

IN calculations of the electron-drift velocity versus electric-field characteristic for GaAs,[1-5] it is assumed that the $\langle 100 \rangle$ or X_1 valleys are the second lowest conduction-band valleys. Thus, electrons which become "hot" in the high-mobility $\langle 000 \rangle$ valley scatter into the low-mobility $\langle 100 \rangle$ valleys and create a bulk negative differential resistance. However, there is little experimental evidence which supports this assumption, and many energy-band calculations predict that the $\langle 111 \rangle$ or L_1 valleys are the second lowest valleys.

Resistivity and Gunn-effect threshold measurements as a function of uniaxial stress have been made on n-type GaAs. The results of these measurements confirm that the $\langle 100 \rangle$ valleys are the second lowest conduction-band valleys.

Previous measurements[6] of the Gunn-effect threshold field in GaAs as a function of uniaxial stress yielded X_1-valley deformation potentials which were considerably different than the values obtained in Si, Ge, and GaP.[7-16] The X_1-valley deformation potential

determined from the measurements reported here are in better agreement with the values in other semiconductors.

II. EXPERIMENTAL TECHNIQUES

A. Sample Preparation

Two types of single-crystal GaAs wafers were used for the uniaxial stress measurements: undoped horizontal boat-grown GaAs which was purchased from the Monsanto Company and tin-doped liquid epitaxial GaAs which was grown at Stanford. The details of the liquid epitaxial crystal growth have been described previously.[17]

Van der Pauw measurements[18] were made on all of the GaAs wafers. A plot of the carrier concentration versus reciprocal temperature for a typical wafer of each type of material is shown in Fig. 1. The carrier concentration of the liquid epitaxial GaAs is almost constant with temperature, thus, the electron concentration is controlled by a shallow donor impurity which remains completely ionized at 77°K. The carrier concentration of the boat-grown GaAs changes several orders of magnitude with temperature, thus, the electron concentration is controlled by a high density of deep-level impurities. The slope of n versus $1/T$ (Fig. 1) yields an ionization energy of $\mathcal{E}_d = 0.21$ eV for the deep level. The electron concentration at the highest temperature is 7×10^{15} cm^{-3}, and the curve shows no indication of saturating (i.e., $n = N_d$), thus, $N_d \gg 1 \times 10^{16}$ cm^{-3}.

The crystallographic orientation of all of the wafers used for the uniaxial stress measurements was checked with an x-ray goniometer. All of the wafers were within $\pm 0.5°$ of a $\langle 100 \rangle$, $\langle 110 \rangle$, or $\langle 111 \rangle$ axis. The oriented

* Permanent address: North American Rockwell Science Center, Thousand Oaks, Calif. 91360.
† Permanent address: Fairchild Semiconductor, Palo Alto, Calif. 94304.
[1] P. N. Butcher and W. Fawcett, Proc. Phys. Soc. (London) 86, 1205 (1965).
[2] P. N. Butcher and W. Fawcett, Phys. Letters 21, 489 (1966).
[3] E. M. Conwell and M. O. Vassell, Trans. IEEE ED-13, 22 (1966).
[4] E. M. Conwell and M. O. Vassell, Phys. Rev. 166, 797 (1968).
[5] A. D. Boardman, W. Fawcett, and H. D. Rees, Solid State Commun. 6, 305 (1968).
[6] M. Shyam, J. W. Allen, and G. L. Pearson, Trans. IEEE ED-13, 63 (1966).
[7] H. Brooks, Advances in Electronics (Academic Press Inc., New York, 1956), Vol. 7, p. 85.
[8] D. Long, Phys. Rev. 120, 2024 (1960).
[9] W. E. Krag, W. H. Kleiner, H. J. Zeiger, and S. Fishler, J. Phys. Soc. Japan Suppl. 21, 230 (1966).
[10] J. E. Aubrey, W. Gubler, T. Henningsen, and S. H. Koenig, Phys. Rev. 130, 1667 (1963).
[11] R. Ito, H. Kauamura, and M. Fukai, Phys. Letters 13, 26 (1964).
[12] I. Balsev, Phys. Rev. 143, 636 (1966).
[13] K. Bulthuis, Philips Research Repts. 23, 25 (1968).

[14] G. Weinreich, T. M. Sanders, Jr., and H. G. White, Phys. Rev. 114, 33 (1959).
[15] H. Fritysche, Phys. Rev. 115, 336 (1959).
[16] I. Balsev, J. Phys. Soc. Japan Suppl. 21, 101 (1966).
[17] J. S. Harris and W. L. Snyder, Solid State Electron. 12, 373 (1969).
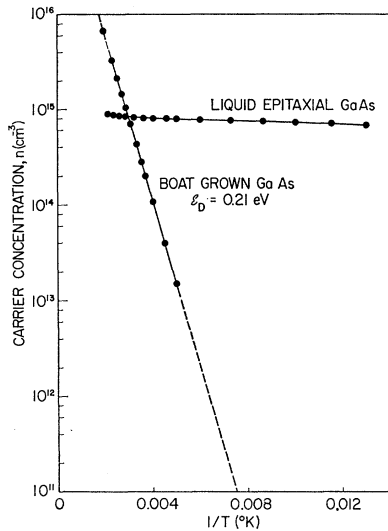[18] L. J. van der Pauw, Philips Research Repts. 13, 1 (1958).

FIG. 1. Electron concentration as a function of reciprocal temperature from Hall measurements on liquid epitaxial and horizontal boat-grown GaAs crystals.

crystals were mechanically lapped and polished to obtain wafers with flat and parallel faces about 150 μm thick. The wafers were degreased in organic solvents and etched in 1 Br:50 methanol for 1 min. Au-Ge-Ni contacts were vacuum evaporated and then alloyed for 30 sec at 440°C in an H_2 atmosphere.[19,20] The wafers were cut into 250×250-μm squares with a wire saw and the sides of the diodes were etched in $3H_2SO_4:1H_2O_2:1H_2O$ to remove any sawing damage.

The electrical characteristics of the diodes were measured at both low and high values of electric field. The criteria for selecting diodes for the uniaxial stress measurements were the following: (a) The low field resistance was within ±15% of the value calculated from the diode dimensions and measured resistivity, and (b) the Gunn-threshold field was between 3000 and 3500 V/cm and the oscillations were coherent with either bias polarity.

B. Uniaxial Stress Apparatus

Uniaxial stress was applied to the diodes with the apparatus shown schematically in Fig. 2. The diode was mounted between a steel disk and steel plate. Both the disk and plate were oil-hardened and polished to provide extremely hard flat surfaces for applying the stress. About 1000 Å of Sn was evaporated onto the disk and plate to insure uniform stress and to provide good electrical contact to the diodes. The stress orientation was determined by the crystallographic orientation of the diodes since the stress was always perpendicular to the contact surfaces. The magnitude of the uniaxial
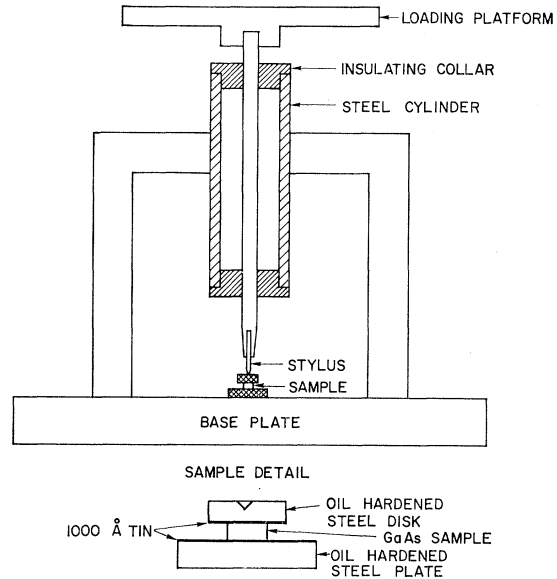
[19] N. Braslau, J. B. Gunn, and J. L. Staples, Solid State Electron. 10, 381 (1967).
[20] J. S. Harris, Y. Nannichi, G. F. Day, and G. L. Pearson, J. Appl. Phys. 40, 4575 (1969).

FIG. 2. Uniaxial stress apparatus. The steel disk is 600 μ in diameter and the samples were typically 250×250 μ in cross section and 100 μ in thickness.

stress was obtained from the static load divided by the diode area. The electrical current was parallel to the stress in all cases.

The electrical measurements were made with the circuit shown in Fig. 3. The two resistors were thin-film stripline resistors connected to the stress apparatus. The voltage pulses were 50 nsec long at a repetition rate of 50 pulses/sec. The voltages V_A and V_B were measured about 40 nsec after the leading edge of the pulse to avoid the initial circuit ringing due to the mismatched load. Low field resistance, Gunn-threshold field and peak drift velocity were determined from the V_B-versus-V_A data on the X-Y recorder.

III. EXPERIMENTAL RESULTS

A. Horizontal Boat-Grown GaAs

The low field resistance as a function of uniaxial stress is shown in Fig. 4. The results of the hydrostatic measurements on similar boat-grown GaAs by Hutson
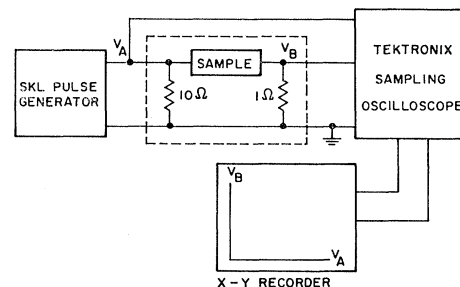

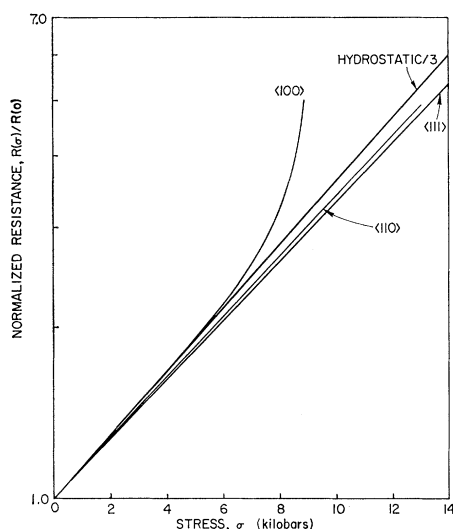FIG. 3. Electrical test circuit for Gunn diodes.

FIG. 4. Normalized diode resistance as a function of stress for horizontal boat-grown GaAs. The magnitude of the hydrostatic pressure has been divided by 3 [see Hutson et al. (Ref. 21)].

et al.[21] are also shown. The magnitude of the hydrostatic pressure has been divided by 3 to compare the hydrostatic and uniaxial data. The increase in resistivity for uniaxial stresses less than 6 kbar was independent of the stress orientation and is in good agreement with the hydrostatic results. The change in resistivity for the $\langle 110 \rangle$ and $\langle 111 \rangle$ diodes remained in agreement with the hydrostatic results until the diodes fractured at approximately 14 and 18 kbar, respectively. However, the $\langle 100 \rangle$ diodes showed an abrupt increase in resistivity for stresses greater than 7 kbar.

The high-electric-field measurements (i.e., Gunn-effect threshold field and peak electron-drift velocity) were impossible to interpret quantitatively because the electron concentration changed as a function of
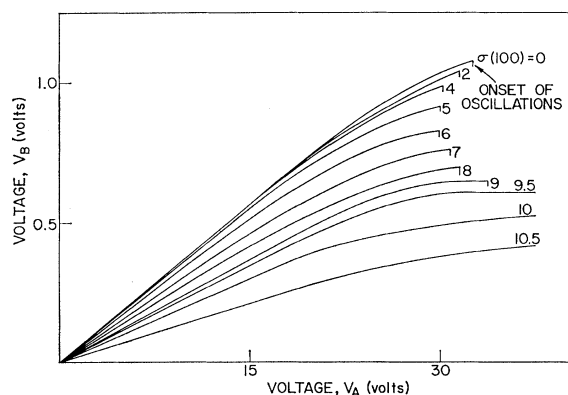

FIG. 5. Typical current-versus-voltage data with $\langle 100 \rangle$ uniaxial stress as a parameter. V_B is the voltage across the current sampling resistor and V_A is the voltage across both the sample and current resistor. No oscillations were observed for $\sigma \geqslant 9.5$ kbar.

A. R. Hutson, A. Jayaraman, and A. S. Coriell, Phys. Rev. **155**, 786 (1967).

stress. Current oscillations were observed for all values of $\langle 111 \rangle$ and $\langle 110 \rangle$ stresses, and for $\langle 100 \rangle$ stresses less than 7 or 8 kbar. However, the oscillations were so nearly quenched at the highest values of $\langle 111 \rangle$ and $\langle 110 \rangle$ stress that it was impossible to conclude that the oscillations in the $\langle 100 \rangle$ diodes were quenched by the decrease in the energy separation of the $\langle 000 \rangle$ and $\langle 100 \rangle$ valleys. The nl product (carrier concentration ×length) of the diodes at the highest values of stress was reduced to about 5×10^{11} cm^{-2}, which is about the value at which traveling dipole domains are unable to form.[22]

B. Liquid Epitaxial GaAs

The stress measurements on the liquid epitaxial GaAs were not plagued by the change in resistance at low values of uniaxial stress. A set of current-versus-voltage curves with $\langle 100 \rangle$ stress as a parameter are shown in Fig. 5. Only the high-field region changed when the stress was less than 6 kbar, and at 9.5 kbar the diode current remained saturated up to electric fields equal to twice the zero-stress threshold field $E_T(0)$. Similar measurements on $\langle 111 \rangle$ diodes showed very little change up to the point of fracture.

The low field resistance as a function of $\langle 100 \rangle$ and $\langle 111 \rangle$ uniaxial stress and hydrostatic pressure is shown in Fig. 6. To insure that the observed changes were not due to plastic deformation or irreversible damage to the crystal, the measurements were repeated as the load was removed. The resistivity change was reversible up to 9 kbar of $\langle 100 \rangle$ stress. At stresses greater than 9 kbar, the samples broke while trying to reduce the load. However, several samples were stressed between 9 and 10.5 kbar for 15 min and no change in resistivity with time was observed. Thus, the increase in resistivity was probably due to an energy-band change caused by elastic strain, which is reversible.

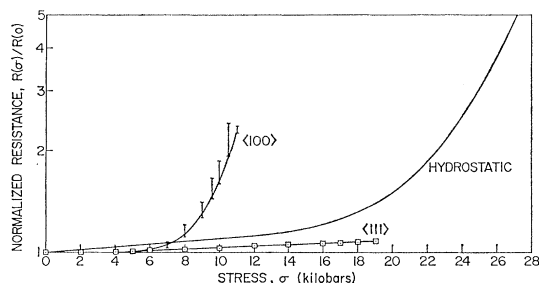The high field results are shown in Figs. 7 and 8. The threshold field (Fig. 7) and peak drift velocity

FIG. 6. Normalized diode resistance as a function of stress for liquid epitaxial GaAs. The vertical bars on the $\langle 100 \rangle$ data show the variation between different diodes. The $\langle 111 \rangle$ samples were nearly identical. The hydrostatic-pressure measurements were made on sulfur-doped horizontal boat-grown GaAs [see Hutson et al. (Ref. 21)].

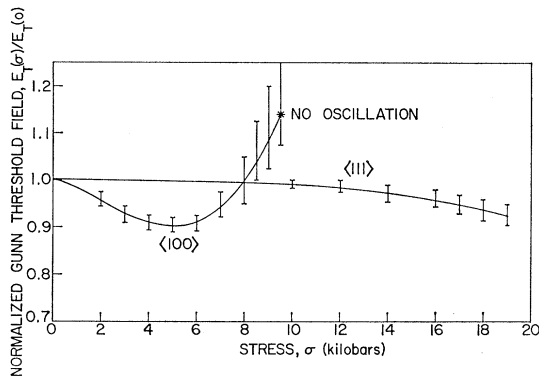H. Kroemer, Proc. IEEE **52**, 1736 (1964).

FIG. 7. Normalized Gunn-threshold field as a function of uniaxial stress. The vertical bars show the variation between different diodes and the uncertainty in determining the threshold field.
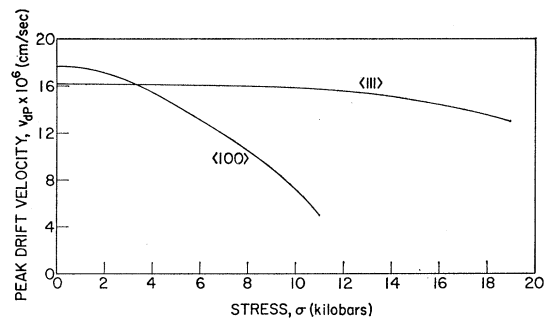

FIG. 8. Peak drift velocity as a function of uniaxial stress. Typical values for 1 sample in each orientation. The peak drift velocity is calculated from the current at $V = V_T$.

(Fig. 8) versus stress were inferred from the current-versus-voltage data on samples which oscillated. The negative differential resistance is small in the $\langle 100 \rangle$ diodes when more than 7 kbar of stress was applied; thus, the amplitude of the oscillations was small and the diodes were noisy. The poor quality of the oscillations at high $\langle 100 \rangle$ stresses made it difficult to determine the Gunn-threshold field and resulted in a large variation between diodes (Fig. 7). The inferred threshold field and peak drift velocity may be less than the actual values, as any inhomogeneity in the diodes would result in current oscillations at an average electric field which is less than the actual threshold field.

IV. DISCUSSION

Figure 9 is a schematic representation of the conduction band of GaAs under uniaxial stress. The solid and dashed curves represent the undeformed energy bands at atmospheric pressure and the deformed energy bands at 10 kbar of uniaxial stress, repectively.

The conduction-band minimum is at the center of the Brillouin zone ($\mathbf{k} = 0$) and about 1.38 eV above the valence band. The next highest minima are at the edges of the Brillouin zone in the $\mathbf{k} = [100]$ directions and about 0.33 eV above the $\mathbf{k} = 0$ band minimum.[23-27] The $\langle 100 \rangle$ valleys are threefold degenerate with no applied stress and with $\langle 111 \rangle$ uniaxial stress. When $\langle 100 \rangle$ and $\langle 110 \rangle$ uniaxial stress are applied, the degeneracy is reduced to a single level and a twofold-degenerate level.

Also shown are the positions of the Fermi energy, the ground-state energy levels for both shallow and deep donors with respect to the conduction-band minimum, and a deep donor with respect to the $\langle 100 \rangle$ valleys. Nonhydrogenic deep impurity levels which are associated with more energetic secondary conduction-band valleys have been considered theoretically,[28,29] and Foyt et al.[30] postulated that such impurity levels were responsible for the exponential increase in resisitivity in CdTe under moderate values of hydrostatic pressure. The energies of both of the deep-level impurities (i.e., one associated with each band minima) are assumed to remain constant with respect to the valence band under the application of uniaxial stress. This assumption is based upon experiments on deep-level donors in GaAs,[21] Si, and Ge, in which the deep-level energies remained constant with respect to the valence band under the application of hydrostatic pressure.

The mechanisms responsible for a change in electron concentration with uniaxial stress are summarized as
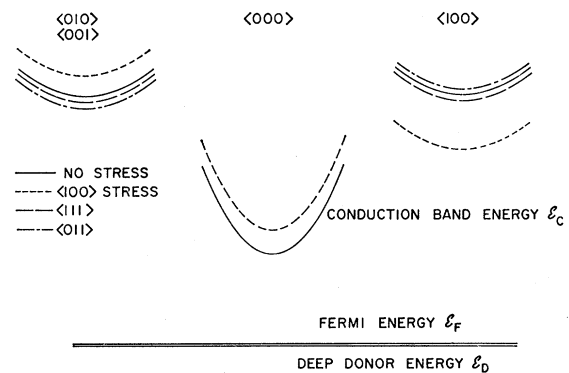
FIG. 9. Energy-band structure of GaAs as a function of uniaxial stress. The deep-impurity level and Fermi energy remain fixed to the valence band when uniaxial stress is applied.

[23] R. C. Eden, J. L. Moll, and W. E. Spicer, Phys. Rev. Letters **18**, 15 (1967).

[24] L. W. James, R. C. Eden, J. L. Moll, and W. E. Spicer, Phys. Rev. **174**, 909 (1968).

[25] L. W. James, Ph.D. thesis, Stanford University, 1969 (unpublished); and private communication.

[26] L. W. James, J. L. Moll, and W. E. Spicer, in *Proceedings of the International Symposium on GaAs, Dallas, 1968* (Institute of Physics and the Physical Society, London, 1969), p. 230.

[27] F. Herman, R. L. Kortum, C. D. Kuglin, J. P. Van Dyke, and S. Skillman, in *Methods of Computational Physics*, edited by B. Adler, S. Fernbach, and M. Rotenberg (Academic Press Inc., New York, 1968), Vol. 8.

[28] G. A. Peterson, in *Proceedings of the International Conference on the Physics of Semiconductors, Paris, 1964* (Dunod Cie., Paris, 1964), p. 771.

[29] H. Kaplan, J. Phys. Chem. Solids **24**, 1593 (1963).

[30] A. G. Foyt, R. E. Holstead, and W. Paul, Phys. Rev. Letters **16**, 55 (1966).

follows:

(a) Electron trapping by a deep-level impurity associated with the conduction-band minimum. The trapping results in an exponential increase in resistance for all values of stress and is isotropic with respect to stress orientation.

(b) Electron trapping by a deep-level impurity associated with the $\langle 100 \rangle$ valleys. This trapping results in an exponential increase in resistance above a certain threshold stress and is isotropic with respect to stress orientation. The threshold stress is the value of stress required to raise the conduction-band minimum above the impurity level.

(c) Electron transfer to a more energetic conduction-band valley in the $\langle 100 \rangle$ direction. The transfer results in an exponential increase in resistance above a threshold value of stress. This threshold is lowest for $\langle 100 \rangle$ stress and highest for $\langle 111 \rangle$ stress.

A. Horizontal Boat-Grown GaAs

The carrier concentration of the boat-grown GaAs is controlled by a high concentration of deep-level impurities which are 0.21 eV below the conduction-band minimum (Fig. 1). Since the electron concentration at 300°K was 2×10^{14} cm^{-3}, the Fermi energy $\mathscr{E}_F$ is nearly equal to the donor ionization energy $\mathscr{E}_D = 0.21$ eV. If this deep level remains fixed to the valence band with with the application of uniaxial stress, then the Fermi level is pinned at this energy. Thus, the energy difference $\mathscr{E}_C - \mathscr{E}_F$ results in a loss of conduction electrons and an increase in resistivity. The rate of change of the energy $\mathscr{E}_C - \mathscr{E}_F$ with stress σ is obtained from the resistivity ρ through the relations

$$\rho(\sigma) = 1/n(\sigma)q\mu \qquad (4.1)$$

and

$$n(\sigma) = N_c \exp\{-[\mathscr{E}_C(\sigma) - \mathscr{E}_F(\sigma)]/kT\}. \qquad (4.2)$$

If the Fermi energy remains fixed to the valence band with stress, then $\mathscr{E}_F(\sigma) = \mathscr{E}_F$ and the rate of change of the energy separation with stress $d[\mathscr{E}_C(\sigma) - \mathscr{E}_F]/d\sigma$ is equal to the change of the forbidden gap energy with stress $d\mathscr{E}_g/d\sigma$. Substituting (4.2) into (4.1) and normalizing,

$$\frac{R(\sigma)}{R(0)} = \frac{\rho(\sigma)}{\rho(0)} = \exp\left(-\frac{\mathscr{E}_C(\sigma) - \mathscr{E}_C(0)}{kT}\right) \qquad (4.3)$$

and

$$\frac{d\mathscr{E}_C}{d\sigma} = \frac{d\mathscr{E}_g}{d\sigma} = kT \frac{d}{d\sigma} \frac{\ln R(\sigma)}{R(0)}. \qquad (4.4)$$

For $\sigma \leqslant 7$ kbar, the resistivity change is isotropic and the slope of $\ln[R(\sigma)/R(0)]$ versus stress (Fig. 4) yields a value of $d\mathscr{E}_C/d\sigma = 3.4 \times 10^{-3}$ eV/kbar of uniaxial stress of 7.8 eV/(unit dilation), independent of orientation. These values are in agreement with values of $d\mathscr{E}_g/dP = 10.6 \times 10^{-3}$ eV/kbar of hydrostatic pressure

or 8.15 eV/(unit dilation).[21] (The volume change of the unit cell is a factor of 3 greater for hydrostatic pressure than for uniaxial stress, thus, the change in $\mathscr{E}_g$/unit uniaxial stress is $\frac{1}{3}$ the change in $\mathscr{E}_g$/unit hydrostatic pressure.)

For stress greater than 7 kbar, the change in resistivity is anisotropic. A second conduction-band valley which is in the $\langle 100 \rangle$ direction, and which decreases in energy with increasing $\langle 100 \rangle$ uniaxial stress, is required to explain the anisotropy (Fig. 9). For $\langle 100 \rangle$ stress greater than 7 kbar, the energy separation of the $\langle 000 \rangle$ and $\langle 100 \rangle$ valleys, $\Delta\mathscr{E}$ is reduced sufficiently that some of the $\langle 000 \rangle$ electrons transfer to the $\langle 100 \rangle$ valley, thus, increasing the resistance. For $\langle 111 \rangle$ and $\langle 110 \rangle$ stresses, the value of $\Delta\mathscr{E}$ remains too large for any significant electron transfer at low electric fields. Deep-level impurities associated with the $\langle 100 \rangle$ valley appear to be unimportant in the electron transfer at high values of stress because the change in resistance is anisotropic and the Gunn oscillations were quenched only by $\langle 100 \rangle$ stress.

B. Liquid Epitaxial GaAs

The conduction-band model for the liquid epitaxial GaAs is the same as that shown in Fig. 9 except there are no deep-level impurities. Thus, the Fermi level is not pinned at a fixed energy with respect to the valence band and it is free to move with the conduction band when stress is applied. The only change in resistance at low values of stress is due to a change in the conduction-band effective mass.[21]

The resistance data for the uniaxial stress and hydrostatic pressure measurements are analyzed with the model proposed by Allen.[6,31] The change in resistance with stress is due to a change in the relative numbers of electrons in the $\langle 000 \rangle$ and $\langle 100 \rangle$ valleys. The mobilities μ_1 and μ_2 are assumed to be constant with stress. The resistivity as a function of stress is

$$\rho(\sigma) = 1/[q(n_1(\sigma)\mu_1 + n_2(\sigma)\mu_2)], \qquad (4.5)$$

where

$$n_2(\sigma)/n_1(\sigma) = (N_2/N_1) \exp[-\Delta\mathscr{E}(\sigma)/kT] \qquad (4.6)$$

and

$$n = n_1 + n_2 = \text{const}. \qquad (4.7)$$

$\Delta\mathscr{E}(\sigma)$ is the energy separation of the $\langle 000 \rangle$ and $\langle 100 \rangle$ valleys, and N_2/N_1 is the density-of-states ratio of the valleys and depends upon the stress orientation.

The hydrostatic measurements[21] were analyzed assuming a density-of-states ratio of 70, which yielded $\Delta\mathscr{E}(0) = 0.36$ eV. Photoemission measurements[23-26] indicate that $0.29 \leqslant \Delta\mathscr{E}(0) \leqslant 0.33$ eV at 300°K. Thus, if $\Delta\mathscr{E}(0) = 0.33$ eV is used to analyze the hydrostatic data, a density-of-states ratio of 40 is obtained. This value is reasonably consistent with the estimates from energy-band calculations for GaAs.[27] Since the $\langle 100 \rangle$

---

[31] J. W. Allen (private communication).

valleys remain degenerate for hydrostatic and $\langle 111 \rangle$ stress, the ratio remains constant; however, $\langle 100 \rangle$ stress lifts the degeneracy and the density of states is reduced by a factor of 3.

With no applied stress, all of the electrons are in the $\langle 000 \rangle$ valley, thus, normalizing Eq. (4.5) yields

$$\frac{\rho(\sigma)}{\rho(0)} = \frac{1 + n_2(\sigma)/n_1(\sigma)}{1 + (\mu_2/\mu_1)[n_2(\sigma)/n_1(\sigma)]}. \quad (4.8)$$

If $n_2(\sigma)/n_1(\sigma) \lesssim 3$, the second term in the denominator can be neglected because $\mu_2/\mu_1 \cong 0.0165$, and Eq. (4.8) reduces to

$$\rho(\sigma)/\rho(0) = 1 + (N_2/N_1) \exp[-\Delta\mathscr{E}(\sigma)/kT]. \quad (4.9)$$

The energy difference between the $\langle 000 \rangle$ valley and a second valley in the i direction is, to first order,

$$\Delta\mathscr{E}^i = \Delta\mathscr{E}_0{}^i + \sum_{m,n} \alpha_{mn}{}^i \epsilon_{mn}, \quad (4.10)$$

where $\Delta\mathscr{E}_0{}^i$ is the energy difference with no applied strain, and m,n run over the crystallographic directions 1, 2, and 3. Since it is impossible to measure strain, it is necessary to obtain an expression for $\Delta\mathscr{E}^i$ as a function of stress σ_{mn} which is known. The relation is

$$\Delta\mathscr{E}^i = \Delta\mathscr{E}_0{}^i + \sum_{m,n} \beta_{mn}{}^i \sigma_{mn}. \quad (4.11)$$

The six $\alpha_{mn}{}^i$ and six $\beta_{mn}{}^i$ coefficients are related through either the 36 compliance or 36 stiffness coefficients. The relation is greatly simplified because GaAs is a cubic crystal, thus, there are only three independent compliance or stiffness coefficients.

The number of $\alpha_{mn}{}^i$ and $\alpha_{mn}{}^i$ coefficients decreases when the $\langle 100 \rangle$ valleys are selected. All of the shear terms ($\alpha_{mn}{}^1$ or $\beta_{mn}{}^1$, where $m \neq n$) are zero by symmetry: i.e., the energy change in a $\langle 100 \rangle$ valley is the same for a plus or minus shear. Transverse symmetry requires that $\alpha_{22}{}^1 = \alpha_{33}{}^1$ and $\beta_{22}{}^1 = \beta_{33}{}^1$, thus, there are only 2 independent coefficients. The energy separations of the $\langle 000 \rangle$ and different $\langle 100 \rangle$ valleys as a function of stress are

$$\Delta\mathscr{E}^1 = \Delta\mathscr{E}_0 + \beta_1 \sigma_1 + \beta_2 (\sigma_2 + \sigma_3),$$
$$\Delta\mathscr{E}^2 = \Delta\mathscr{E}_0 + \beta_1 \sigma_2 + \beta_2 (\sigma_1 + \sigma_2),$$
$$\Delta\mathscr{E}^3 = \Delta\mathscr{E}_0 + \beta_1 \sigma_3 + \beta_2 (\sigma_1 + \sigma_2),$$

where the notation for $\Delta\mathscr{E}^i$, β_i, and σ_i follow the notation of Nye[32] and $i = 1, 2, 3$ correspond to crystallographic directions: $1 \leftrightarrow \langle 100 \rangle$, $2 \leftrightarrow \langle 010 \rangle$, and $3 \leftrightarrow \langle 001 \rangle$. An analogous expression for $\Delta\mathscr{E}^i$ as a function of the strains ϵ_{mn} can be obtained from Eq. (4.10).

If a compressive stress $(-\sigma)$ is applied, the stress components and energy separation between the $\langle 000 \rangle$

valley and different $\langle 100 \rangle$ valleys are as follows:

(a) $\langle 100 \rangle$ uniaxial stress:

$$\sigma_1 = -\sigma,$$
$$\sigma_2 = \sigma_3 = 0,$$
$$\Delta\mathscr{E}^1 = \Delta\mathscr{E}_0 - \beta_1 \sigma_1,$$
$$\Delta\mathscr{E}^2 = \Delta\mathscr{E}^3 = \Delta\mathscr{E}_0 - \beta_2 \sigma.$$

(b) $\langle 110 \rangle$ uniaxial stress:

$$\sigma_1 = \sigma_2 = -\tfrac{1}{2}\sigma,$$
$$\sigma_3 = 0,$$
$$\Delta\mathscr{E}^1 = \Delta\mathscr{E}^2 = \Delta\mathscr{E}_0 - \tfrac{1}{2}\sigma (\beta_1 + \beta_2),$$
$$\Delta\mathscr{E}^3 = \Delta\mathscr{E}_0 - \tfrac{1}{2}\beta_2 \sigma.$$

(c) $\langle 111 \rangle$ uniaxial stress:

$$\sigma_1 = \sigma_2 = \sigma_3 = -\tfrac{1}{3}\sigma,$$
$$\Delta\mathscr{E}^1 = \Delta\mathscr{E}^2 = \Delta\mathscr{E}^3 = \Delta\mathscr{E}_0 - \tfrac{1}{3}\sigma (\beta_1 + 2\beta_2).$$

(d) hydrostatic pressure:

$$\sigma_1 = \sigma_2 = \sigma_3 = -\sigma,$$
$$\Delta\mathscr{E}^1 = \Delta\mathscr{E}^2 = \Delta\mathscr{E}^3 = \Delta\mathscr{E}_0 - \sigma (\beta_1 + 2\beta_2).$$

A best fit to the experimental-resistivity–versus–stress data (Fig. 6) is obtained with $\beta_1 = 2.1 \times 10^{-2}$ eV/kbar and $\beta_2 = -0.50 \times 10^{-2}$ eV/kbar. The α_i coefficients calculated from these β_i coefficients are

$$\alpha_1 = c_{11}\beta_1 + 2c_{12}\beta_2 = 19.5 \text{ eV}$$

and

$$\alpha_2 = c_{12}\alpha_1 + (c_{12} + c_{11})\beta_2 = 2.7 \text{ eV}.$$

The coefficients α_1 and α_2 are related to the deformation potential parameters $\Xi_u{}^1$ and $\Xi_d{}^1$ introduced by Herring and Vogt.[33,34] For $\langle 100 \rangle$ valleys, $\Xi_d{}^1$ is the energy change due to dilatation and $\Xi_u{}^1$ is the energy shift due to uniaxial strain. The change in the $\langle 000 \rangle$ valley energy must be included since $\Xi_u{}^1$ and $\Xi_d{}^1$ only pertain to the $\langle 100 \rangle$ valleys and α_1 and α_2 describe the energy difference between the $\langle 000 \rangle$ and $\langle 100 \rangle$ valleys. From the uniaxial-stress measurements on boat-grown GaAs, the change in the $\langle 000 \rangle$ valley per unit strain is $\Xi_d{}^0 = 7.8$ eV. The change in $\Delta\mathscr{E}^1$ is

$$\Delta\mathscr{E}^1 = \Delta\mathscr{E}_0 + \alpha_1 \epsilon_1 + \alpha_2 (\epsilon_2 + \epsilon_3)$$
$$= \Delta\mathscr{E}_0 + \Xi_d{}^0 (\epsilon_1 + \epsilon_2 + \epsilon_3) + \Xi_u{}^1 \epsilon_1 + \Xi_d{}^1 (\epsilon_1 + \epsilon_2 + \epsilon_3)$$
$$= \Delta\mathscr{E}_0 + (\Xi_d{}^0 + \Xi_d{}^1 + \Xi_u{}^1)\epsilon_1 + (\Xi_d{}^0 + \Xi_d{}^1)(\epsilon_2 + \epsilon_3).$$

Therefore,

$$\Xi_d{}^1 = \alpha_2 - \Xi_d{}^0 = -5.1 \text{ eV}$$

and

$$\Xi_u{}^1 = \alpha_1 - \Xi_d{}^0 - \Xi_d{}^1 = \alpha_1 - \alpha_2 = 16.8 \text{ eV}.$$

Thus, the deformation potentials for the $\langle 100 \rangle$ valleys in GaAs are $\Xi_u{}^1 = 16.8$ eV and $\Xi_d{}^1 = -5.1$ eV. These deformation potentials are about the same magnitude

[32] J. F. Nye, *Physical Properties of Crystals* (Oxford University Press, London, 1957).

[33] C. Herring, Bell System Tech. J. **34**, 237 (1955).
[34] C. Herring and E. Vogt, Phys. Rev. **101**, 944 (1956).

as those of the $\langle 100 \rangle$ valleys in Si and the $\langle 111 \rangle$ valleys in Ge. For Si, $\Xi_u = 9.2$ eV and $\Xi_d = -1.4$ eV, and, for Ge, $\Xi_u = 19.2$ eV and $\Xi_d = -10.5$ eV.[7,11-15]

These deformation potentials for the $\langle 100 \rangle$ valleys in GaAs ($\Xi_u = 16.8$ eV and $\Xi_d = -5.1$ eV) have been inserted into Conwell's[4] Eqs. (4.2) and (4.4) to calculate the electron mobility due to acoustic phonon scattering for electrons in the $\langle 100 \rangle$ valleys. The calculated lattice mobility is $\mu_L = 600$ cm²/V sec. This mobility was combined with the mobility limited by other scattering mechanisms to obtain a total mobility for electrons in the $\langle 100 \rangle$ valleys of $\mu_2 = 120$ cm²/V sec. This value is in agreement with the measured $\langle 100 \rangle$ electron mobility, 110 cm²/V sec.[21]

V. CONCLUSIONS

The electrical-resistivity measurements in GaAs as a function of temperature and uniaxial stress reveal two distinct types of behavior depending upon the source of the GaAs crystals. The two types of behavior are the limiting cases for GaAs in which the electrical properties are dominated by (1) a high concentration of deep-level impurities and traps, and (2) a moderate concentration of shallow-level impurities which remained completely ionized in these experiments.

The resistivity and Gunn-effect threshold measurements as a function of uniaxial stress provide experimental evidence that the $\langle 100 \rangle$ or X_1 valleys are the secondary conduction-band valleys in GaAs. Utilizing the recently measured value for $\Delta\mathcal{E} = 0.33$ eV,[25,26] the ratio of the densities of states is $N_2/N_1 = 40$ and the deformation potential for the $\langle 100 \rangle$ valleys are $\Xi_u^1 = 16.8$ eV/(unit strain), $\Xi_d^1 = -5.1$ eV/(unit strain) and, for the $\langle 000 \rangle$ valley, $\Xi_d^0 = 7.8$ eV/(unit strain). The value of Ξ_d^0 is in agreement with the value obtained by hydrostatic pressure measurements.[21] The calculated mobility of electrons in the $\langle 100 \rangle$ valleys is $\mu_2 = 120$ cm²/V sec which is also in agreement with the measured value of electron mobility[21] in the $\langle 100 \rangle$ valleys.

Optical Double Resonance in Solids

YIZHAK YACOBY

Microwave Division, Department of Physics, Hebrew University, Jerusalem, Israel

(Received 1 April 1969)

Nonlinear interaction of two electromagnetic beams with a semiconducting or insulating crystal is considered under the following conditions: The photon energy $\hbar\Omega$ of an intense laser beam is equal to the gap between two conduction bands $\hbar\Omega_{32}$ at certain points in the crystal momentum space. The photon energy $\hbar\omega$ of a relatively weak beam is approximately equal to the gap between the valence band and one of the conduction bands $\hbar\Omega_{21}$ at the same points in crystal momentum space. These conditions are referred to as double resonance. A theory is developed for two nonlinear effects: (1) the change of the dielectric coefficient of the crystal at frequency ω caused by the Ω perturbation; and (2) the generation of a parametric beam at frequency $\omega + \Omega$. An interesting result of the theory is that both effects are very sensitive to the conditions at the point of contact of the surfaces of constant Ω_{31} and Ω_{21} in K space. The effects obtained when $\partial\Omega_{31}/\partial K_\perp$ and $\partial\Omega_{21}/\partial K_\perp$ have the same sign are much smaller than those obtained when they have opposite signs. ($K_\perp$ is the component of $\mathbf{K}$ perpendicular to the surfaces at the point of contact.) This phenomenon is explained in terms of combined electronic and electromagnetic states. Possible applications of these effects to the investigation of the band structure of solids are discussed. In particular, it is shown that measurements of double-resonance effects will yield information about the band structure at noncritical points in the Brillouin zone.

I. INTRODUCTION

IN recent years, several new optical methods were developed for the investigation of the band structure of solids. Methods which were found very useful in this respect are the electroabsorptance,[1] electroreflectance,[2] piezoreflectance,[3] and others known, in general, as the differential optical methods. These methods consist of measuring the variation in an optical property of the crystal, such as absorption or reflection coefficients, caused by the variation of a parameter, such as an

[1] A. Frova, P. Handler, F. A. Germano, and D. E. Aspnes, Phys. Rev. **145**, 575 (1966); Y. Yacoby, *ibid.* **142**, 445 (1966).

[2] B. O. Seraphin, Phys. Rev. **140**, A1716 (1965); M. Cardona, K. L. Shaklee, and F. H. Pollak, *ibid.* **154**, 696 (1967).

[3] M. Garfinkel, J. J. Tiemann, and W. E. Engeler, Phys. Rev. **148**, 695 (1966).